Original Article

# Histological and Immunohistochemical Study of the Effect of Medical Ozone on Acute Renal Cortical Injury Induced by Shock Wave Lithotripsy in Adult Male Albino Rats

*Nehad F. Mazen, Aisha A. Alkhodary, Sara A. Kandeel and Ebtehal Z. Hassan*

*Department of Medical Histology and Cell Biology, Faculty of Medicine, Zagazig University, Zagazig, Egypt*

## ABSTRACT

**Introduction:** Acute kidney injury (AKI) is caused by the ischemic reperfusion injury brought on by ESWL exposure.

**Aim of the Work:** To study the impact of medicinal ozone on acute renal cortical injury induced by ESWL.

**Material and Methods:** Forty-four adult male Wistar rats were divided into: the control group; subdivided into negative control group (received no treatment) and positive control group (received intra-peritoneal injection of ozone/oxygen combination given once daily at a dose of 1mg/kg), the ESWL group; received 2000 shocks on the right kidney at a power level of 90 to 100% at a rate of 60 shockwaves per minute under X-ray guidance and the ESWL+medical ozone group; received the ozone flow maintained at 3 L/min, equivalent to a gas combination of 97% O2 and 3% O3 with an ozone concentration of 60mg/ml via intra-peritoneal injection. After three days, blood samples were obtained to estimate serum urea and creatinine. Kidney tissues were processed for measurement of malondialdehyde (MDA), superoxide dismutase (SOD) and glutathione peroxidase (GPx), and light and electron microscopic examination. Morphometric and statistical analyses were performed.

**Results:** The ESWL group revealed significantly high levels of serum creatinine and urea and tissue MDA, and decreased SOD and GPx levels. There were shrinkage of glomeruli, distorted feet processes and thick basement membrane. Tubules were distorted with cytoplasmic vacuoles. The area% of collagen fibers and iNOS and HSP-70 immunoreactivity increased while the glomerular diameter decreased. Medical ozone caused marked improvement, both structurally and functionally.

**Conclusion:** Medical ozone can ameliorate ESWL-induced AKI via its antioxidant and anti-inflammatory properties.

**Received:** 07 February 2023, **Accepted:** 23 May 2023

**Key Words:** Acute kidney injury, Hsp-70, ozone, rat, shock wave lithotripsy.

**Corresponding Author:** Ebtehal Z. Hassan, PhD, Department of Medical Histology and Cell Biology, Faculty of Medicine, Zagazig University, Zagazig, Egypt, **Tel.**: +20 10 0124 4853, **E-mail:** ebtehalzaid.81@gmail.com

**ISSN:** 1110-0559, Vol. 47, No. 2

## INTRODUCTION

Acute kidney injury (AKI) is a clinical problem with rising prevalence and insufficient therapy alternatives. It is characterized by a rapid (within hours) deterioration in kidney function accompanied by structural damage[1]. AKI includes prerenal AKI, acute postrenal obstructive nephropathy and intrinsic acute kidney diseases[2].

Intrinsic AKI is considered the most clinically significant subtype in critically ill patients and can be associated with acute tubular necrosis (ATN). Its prognosis remains poor with a mortality rate of 40-80% in the intensive care unit. Its causes are categorized into: glomerular, tubular, vascular and interstitial causes[3].

The glomerular causes include acute inflammation of glomerular blood vessels and deposition of immune complexes especially in the glomerular basement membrane (GBM)[4]. On the other hand, the vascular causes include any acute event that reduces renal perfusion and GFR such as atherosclerotic plaques and cholesterol emboli in renal blood vessels[5]. Clinically, the main cause of intrinsic AKI is ischemia which can be caused by shock waves, hemorrhage and trauma[6].

Extracorporeal shock wave lithotripsy (ESWL) is one of the safest and most effective ways to treat kidney stones. The European Association of Urology approved ESWL as the primary line of treatment for most renal stones under 2 cm in diameter that are situated in the pelvis or upper and middle calyces[7]. It has been a popular therapy option for many people for more than three decades[8].

Two major effects of shock waves on renal tissue can be distinguished: traumatic vascular injury and ischemic reperfusion injury. Each of them has a different pathophysiological background. Acute renal injury following IRI does not improve and typically worsens over time. As an organ with high perfusion rates, the kidney is sensitive to reperfusion following ischemia[9,10].

Medical ozone; oxygen and ozone gas mixture, was proved to be curative in many illnesses, such as peritonitis,

 *DOI: 10.21608/ejh.2023.191377.1851*

infected wounds and severe ischemic diseases[11]. Previous studies proposed different therapeutic properties for medical ozone including antimicrobial, anti-inflammatory and antioxidant effects[12].

Medical ozone increases antioxidant enzyme activities such as superoxide anion by superoxide dismutase (SOD) and hydrogen peroxide by glutathione peroxidase (GPx). Ozone-blood interaction includes several biochemical steps. First, oxygen-ozone gas mixture dissolves in plasma. Ozone reacts mainly with antioxidant and polyunsaturated fatty acids (PUFAs). This results in generation of little concentration of ROS and lipid oxidation products (LOPs)[13].

There is yet no effective way to stop ischemic AKI brought on by ESWL in clinical settings. It is important to find a new clinical strategy for managing AKI and preventing the progress to its complications. Therefore, the objective of our study was to investigate whether medical ozone can ameliorate the histological and biochemical alterations induced by ESWL in the renal cortex of adult male albino rats.

## MATERIALS AND METHODS

### *Animals*

Forty four adult male Wistar albino rats weighing 200-250gm, aged 6-7 weeks were used. They were obtained from the Breading Animal House, Faculty of Medicine, Zagazig University. They were housed in a controlled room (temperature 25-27°C, 12-h light/12-h dark/cycle, and relative humidity of 40-70%) with food and water ad- libitum. They were acclimatized to their environment at least two weeks before starting the experiment. All experimental procedures were performed in accordance with the guidelines of the Institutional Animal Care and Use Committee (ZU-IACUC/F/135/2019 is the protocol approval number), and accepted by the Faculty of Medicine; Zagazig University.

### *Chemicals & instruments*

1. ESWL: Dornier lithotripter S (EMSE 220F XP) (Germany): Zagazig University's Faculty of Medicine's Urology Department.
2. Medical ozone: Ozone is generated at the Rheumatology Department - Faculty of Medicine - Zagazig University using ozone generator (OZONOSAN Photonic 1014, Hans GmbH Nordring and Iffezheim, Germany).

### *Experimental design*

Rats in all groups were anaesthetized via an intra-muscular injection of 50mg/kg ketamine HCL and 10mg/kg xylazine. Laparotomy was performed in all rats under complete aseptic conditions. Following upper abdominal midline incision, one hemo-clip was attached to the peri-renal fatty tissue of right kidney for localization[14].

### *Rats were divided into three main groups*

**Control group** (Group I, 22 rats): they were subdivided into two subgroups (eleven rats each):

- Subgroup Ia: (negative control): rats received no treatment throughout the experiment.
- Subgroup Ib: (positive control): rats received intra-peritoneal injection of ozone/oxygen combination given once daily at a dose of 1mg/kg[15].

ESWL group (Group II, 11 rats): Before the ESWL session, rats received intra-peritoneal injections of 10mg/kg xylazine hydrochloride and 50mg/kg ketamine HCL for anesthesia[14]. Under X-ray guidance, shock waves were administered to the right kidney while the rats were positioned in the supine posture on the lithotripter platform. Using a Dornier lithotripter S (EMSE 220F XP) (Germany), 2000 shocks at a power level of 90 to 100% were delivered to each rat at a rate of 60 shockwaves per minute[16].

ESWL group treated with medical ozone (Group III, 11 rats): rats received the ozone flow which was maintained at 3 Litre/min, equivalent to a gas combination of 97% O2 and 3% O3 with an ozone concentration of 60mg/ml. Following exposure to the ESWL session, an intra-peritoneal (IP) injection of ozone/oxygen combination was administered with a single dose of 1 mg/kg/day for three days in a row[17].

Three days after the experiment began; rats were sacrificed after being given an intra-peritoneal injection of sodium phenobarbital with a dose of 50mg/kg. Blood samples from the orbital vein were collected to measure the serum concentrations of urea and creatinine, and antioxidant enzymes in tissue homogenates[18].

Intra-cardiac perfusion was carried out through the heart apex with 2.5% glutaraldehyde in 0.1 mol/l cacodylate buffer (pH 7.3) for 5 min for partial fixation of the kidney. A midline upper abdominal incision was performed and the kidney was dissected. The samples were prepared for biochemical and histological studies[19].

### *Biochemical analysis*

Serum urea and creatinine levels : Blood was collected in a capillary tube by a retro-orbital puncture from each rat in all groups. The samples were centrifuged at a speed of 3000 rpm to separate the serum. The samples were kept at -20°C in a freezer. Quanti Chrom TM assay kits were used to estimate measurements using a traditional colorimetric approach[20].

Assessment of super-oxide dismutase (SOD) activity: It was measured in a tissue homogenate according to the method described by Nishikimi *et al*[21]. It was achieved relying on the ability of the enzyme to inhibit the phenazine methosulphate mediated reduction of nitroblue tetrazolium dye. The increase in absorbance at 560 nm for 5 min is measured. The results were expressed as U/gm.

Assessment of glutathione peroxidase (GPx) activity: The Paglia and Valentine method was used to calculate GPx in kidney homogenates[22]. The assay is an indirect measure of the activity of cellular GPx. Oxidized glutathione; produced upon reduction of an organic peroxidase by GPx, is recycled to its reduced state by the enzyme glutathione reductase. The tissue homogenate is added to a solution containing glutathione, glutathione reductase and NADH. The oxidation of NADH to NADP+ is accompanied by a decrease in absorbance at 340nm (A340) providing a spectrophotometric means for monitoring GPx enzyme activity. The results were expressed as U/gm.

Assessment of malondialdhyde (MDA) activity: It was determined using the Ohkawa *et al*. technique in kidney homogenates[23]. Thiobarbituric acid (TBA) reacts with MDA in an acidic medium at tempreture 950 C for 30 min to form thiobarbituric acid reactive product. The absorbance of resultant pink product can be measured at 534 min. The results were expressed as nmol MDA/g tissue.

### *Histological study*

The right kidney of each animal was carefully dissected and divided into two parts; one for light and the other for electron microscopic preparations.

### *Light microscopic study*

According to Suvarna *et al*,[24] specimens were immediately fixed in formaldehyde for 24 hours, dehydrated, cleared, impregnated in pure soft paraffin and then embedded in hard paraffin. Serial were cut at 5-µm thickness by a microtome. The sections were stained by the following methods:

1. Hematoxylin & eosin.
2. Mallory trichrome for identification of collagen fibers.
3. Periodic acid Schiff (PAS). To assess brush border of proximal convoluted tubules and basement membranes of renal tubules and glomerular capillaries.
4. Immuno-histochemical staining for:
    a. Inducible nitric oxide synthase (iNOS): a marker for inflammation-induced nitric oxide synthesis[25]. Primary antibody is a mouse monoclonal IgG-type antibody (clone 608, Cat. #M 618, DAKO, Egypt)
    b. Heat shock protein-70 (HSP-70): an indicator of thermal and oxidative stress[26]. Primary antibody is a mouse monoclonal IgG-type antibody (clone 3A3, Cat. # MA3-006, Thermo Fisher Scientific, USA)

In order to prepare the sections for immuno-staining, they were initially placed in a 10 Mm, pH 6 citrate solution to boil for 10 minutes to extract antigens, afterwards 20 minutes of cooling at room temperature. The primary antibodies were applied to the sections for an hour. The immuno-staining procedure was completed with an ultra-vision detecting system, and Mayer's hematoxylin was used as a counter-stain.

### *Electron microscopic study*[27]

Leica ultra-cut (UCT) ultra-thin sections were obtained, analyzed, and photographed using a JOEL EM 1010 transmission electron microscope after staining with uranyl acetate and lead citrate in the Faculty of Agriculture - Mansoura University - Electron Microscope Research Laboratory (EMRL) (Egypt).

### *Morphometric study*

The data were obtained using the Leica QWin 500 image analyzer computer system (Leica Ltd, Cambridge, UK) in the image analysis unit at Pathology Department, Faculty of Dentistry, Cairo University. The image analyzer consisted of a colored video camera, colored monitor and hard disc of IBM personal computer connected to the Olympus microscope (CX 41) and controlled by Leica QWin 500 software. The image analyzer was first calibrated automatically to convert the measurement units (pixels) produced by the image analyzer program into actual micrometer units. The image analyzer computer system was used to evaluate the area percentage of collagen fibers, iNOS and HSP-70 immuno-reaction and diameter of glomeruli. The measuring frame of a standard area was equal to 7286, 78 µm2. For each parameter, ten different non overlapping fields from each slide were examined.

### *Analysis of statistics*

Data were presented as means ± standard deviation (SD). The data were subjected to one-way Analysis of Variance (ANOVA) at 95% level of confidence and the statistical package for social sciences (SPSS-16; Chicago, IL, USA) program. The Tukey's Kramer HD test which considers $p < 0.05$ to be significant and highly significant if $P < 0.001$, was used to identify significant differences between the means[28].

## RESULTS

### *General observation*

The animals in the ESWL group showed petechial hemorrhage on the skin at the site of delivery of shock waves immediately after ESWL session. No macro¬scopic changes were noted in the abdominal organs during exploration (Figure 1).

### *Biochemical results (Table 1, Figure 2 a,b)*

The ESWL group had significantly increased levels of serum creatinine and urea ($P < 0.0001$, $P < 0.0009$, respectively), and MDA in tissue homogenates ($P < 0.013$) while there was decreased SOD and GPx levels in tissue homogenates, compared to the control and medical ozone groups. On the other hand, the difference between the control and medical ozone groups was non-significant.

## *Histological results*

### 1) Light microscopic findings

H&E-stained sections of the control rats revealed intact renal corpuscles and renal tubules. Each renal corpuscle was made up of tuft of capillaries; glomerulus, that was enclosed in Bowman's capsule which consists of visceral and parietal layers and Bowman's space in between. Proximal and distal convoluted tubules were lined by simple cuboidal epithelium with central rounded pale nuclei. The lumina of the PCTs were narrower than the distal ones (Figure 3A).

ESWL group showed glomerular atrophy with wide Bowman's spaces. Also, glomerular vacuolations were observed. Tubules appeared distorted with dark nuclei and vacuolated cytoplasm. The interstitium revealed cellular infiltration, thick congested blood and congested peri-tubular capillaries (Figures 3 B,C).

Medical ozone-treated group showed the renal corpuscles with glomerular capillary tufts surrounded by Bowman's space. Some of the glomeruli were congested. The interstitium showed cellular infiltration and congested peri-tubular capillaries. Most of the epithelial lining cells of the PCTs and DCTs exhibited acidophilic cytoplasm and vesicular nuclei (Figure 3D).

Few collagen fibers around the renal corpuscles, blood vessels and renal tubules were exhibited in Mallory's trichrome-stained sections of the control rats (Figure 4A). ESWL group showed capsular thickening with increased collagen fibers around tubules, glomerular capillaries and blood vessels (Figures 4 B,C). Moderate amount of collagen fibers around the renal corpuscles, blood vessels and renal tubules were observed in medical ozone-treated group (Figure 4D).

The brush borders of PCTs as well as the basement membranes of renal corpuscles, glomerular capillaries and renal tubules, showed positive PAS reaction in sections of the control rats (Figure 5A). In sections of ESWL group, focal loss of reaction in the brush borders of some renal tubules was revealed (Figure 5B). Medical ozone-treated group showed positive reaction at the brush borders of most renal tubules and the basement membranes of renal tubules and glomerular capillaries. Areas of loss of reaction were still detected in some tubules (Figure 5C).

Immune localization of iNOS in the control rats exhibited faint cytoplasmic reaction in few renal tubules and glomeruli (Figure 6A). Most cells lining tubules and glomerular capillaries in sections of the ESWL group had an increased cytoplasmic reaction (Figure 6B). Some of the lining cells of tubules and glomerular capillaries had an increased cytoplasmic reaction in the medical ozone-treated group (Figure 6C).

Immune localization of HSP-70 in the control rats revealed cytoplasmic and nuclear reactions in some lining cells of renal tubules (Figure 7A). ESWL group revealed an increased reaction in the cells lining glomerular capillaries and tubules (Figures 7 B,C). Medical ozone-treated group exhibited positive reaction both in nuclei and cytoplasm of few lining cells of tubules and glomerular capillaries (Figure 7D).

### 2) Electron microscopic findings

Ultrathin sections of the blood renal barrier (BRB) in the control rats showed podocytes with primary and inter-digitating secondary feet processes. Glomerular blood capillaries were lined by thin fenestrated endothelium. The glomerular basement membrane appeared thin and uniform (Figure 8A). ESWL group showed glomerular capillaries with distortion of their endothelial lining, focal loss of fenestration and thick glomerular basement membrane. Podocytes had small heterochromatic nuclei and distorted feet processes (Figure 8B). Medical ozone-treated group showed marked improvement. Glomerular capillary endothelium was thin with intact fenestrations. The glomerular basement membrane appeared thin and uniform. There were regularly arranged feet processes of podocytes. However, some distorted feet processes and areas of lost fenestrations were still observed (Figure 8C).

Regarding the epithelial cells lining PCTs in the control group, they had pale nuclei with prominent nucleoli, intact microvilli, elongated mitochondria lodged within basal infoldings and thin basement membrane (Figure 9A). ESWL group contained apical cytoplasmic vacuolations, autophagosomes, distorted mitochondria, irregular basal infoldings and thick basement membrane (Figures 9 B,C). Medical ozone-treated group revealed pale nuclei, intact microvilli, elongated mitochondria appeared lodged within basal infoldings and thin uniform basement membrane. However, cytoplasmic vacuoles were still present (Figure 9D).

As regards the epithelial cells lining DCTs in the control group, they showed pale nuclei with prominent nucleoli, intact microvilli, elongated mitochondria lodged within basal infoldings, and a thin basement membrane (Figure 10A). ESWL group exhibited small heterochromatic nuclei, irregular mitochondria distorted basal infoldings and a thick basement membrane (Figure 10B). Medical ozone-treated group revealed pale nuclei, elongated mitochondria within their basal infoldings. However, the basement membrane was thick (Figure 10C).

## *Morphometric results and statistical analysis*

The mean values of area% of collagen fibers were significantly higher in the ESWL group compared to the control as *p. value* <0.001 (21.20 ± 9.75and 5.49 ± 1.99 respectively). When compared to the control, the medical ozone treated group exhibited a non-significant difference (Figure 11, Table 2).

Area% of iNOS and HSP-70 immunoreaction mean values exhibited a significantly increase in the ESWL group (13.67 ± 3.78 and 12.43 ± 1.39 respectively) compared to the control group as *P value* <0.0001. There was a non-

significant difference between the medical ozone-treated group and the control group (Figure 11, Table 2).

The diameter of glomeruli showed a significant decline in the ESWL group (0.75 ± 0.19) when compared to control (1.88 ± 0.13) as *P value* <0.0001. On the other hand, a non-significant difference between the medical ozone-treated group (1.76 ± 0.20) and the control group was reported (Figure 11, Table 2).


**Fig. 1:** Petechial hemorrhage on the skin at the site of delivery of shock waves

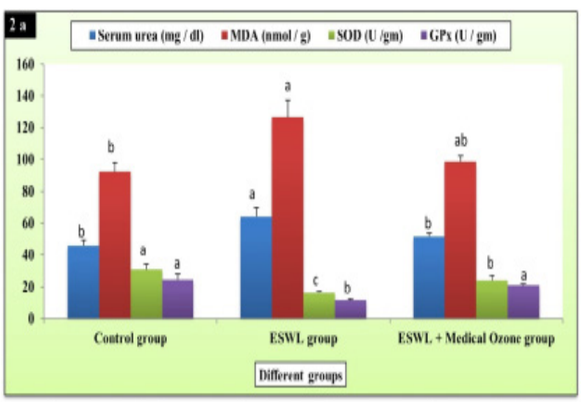


**Fig. 2a:** Changes in serum urea, MDA, SOD and GSPx in different experimental groups

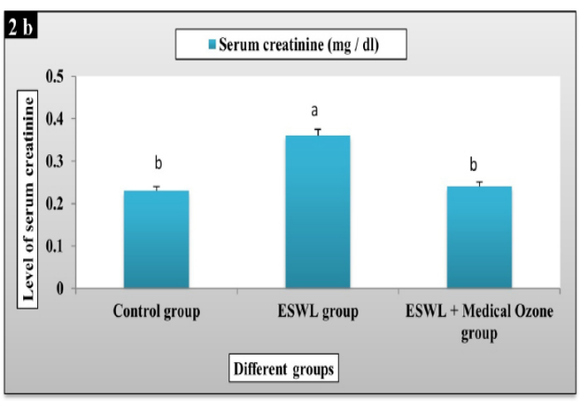


**Fig. 2b:** Changes in serum creatinine levels (mg/dl) in different experimental groups

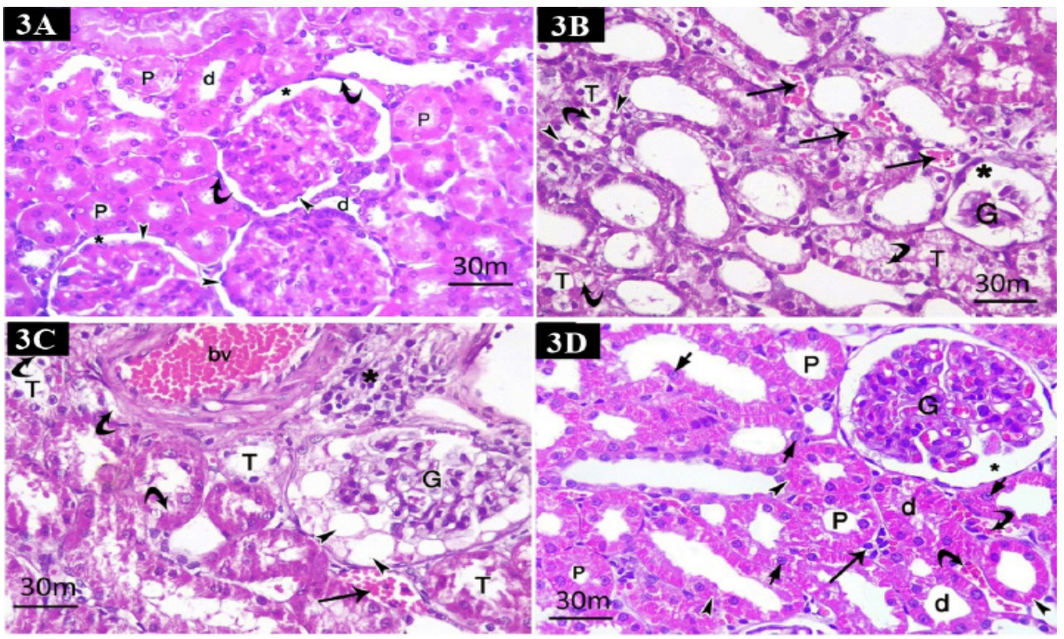


**Fig. 3:** H&E-stained sections in the renal cortex. (A) Control group showing glomeruli surrounded by visceral (arrow head) and parietal (curved arrow) layers of Bowman's capsule that are separated by Bowman's space (asterisk). Proximal (P) and distal (d) convoluted tubules are lined by simple cuboidal epithelium with pale central rounded nuclei. The lumina of the proximal tubules are narrower than the distal ones. (B & C) ESWL group showing in (B), atrophied glomerulus (G) with wide Bowman's space (asterisk). Tubules appear distorted (T) with vacuolated cytoplasm (curved arrow) and dark nuclei (arrow head). Congested peri-tubular capillaries (arrow) are also seen. In (C), showing vacuolated cytoplasm (curved arrow) in some of tubules (T). Glomerular (G) vacuolation is observed (arrow head). The interstitium reveals cellular infiltration (asterisk), a thick congested blood vessel (bv) and congested peritubular capillaries (arrow). (D) ESWL treated with medical ozone group showing congested glomerular capillaries (G) surrounded by Bowman´s space (asterisk). The proximal (P) and distal (d) convoluted tubules are seen with acidophilic cytoplasm (arrow head) and vesicular nuclei (short arrow). The interstitium shows cellular infiltration (arrow) and congested peri-tubular capillaries (curved arrow). (H&E x400)

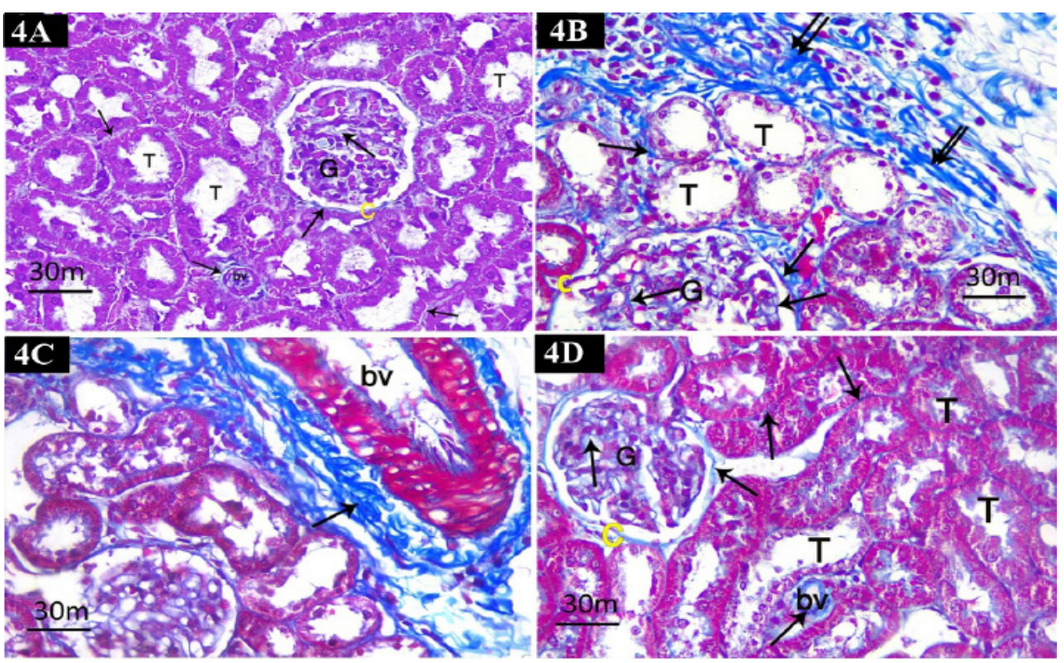


**Fig. 4:** Mallory trichrome-stained sections. (A) Control group showing few collagen fibers (arrow) around the renal corpuscle (C), glomerular capillaries (G) and blood vessels (bv) and in-between renal tubules (T). (B & C) ESWL group showing in (B), thick capsule (double arrow). There are increased collagen fibers (arrows) around tubules (T), renal corpuscle (C) and glomerular capillaries (G). In (C), showing abundant collagen fibers (arrow) around blood vessel (bv). (D) ESWL treated with medical ozone group showing moderate amount of collagen fibers (arrows) around the glomerular capillaries (G), the renal corpuscle (C), the renal tubules (T) and blood vessels (bv). (Mallory trichrome x400)

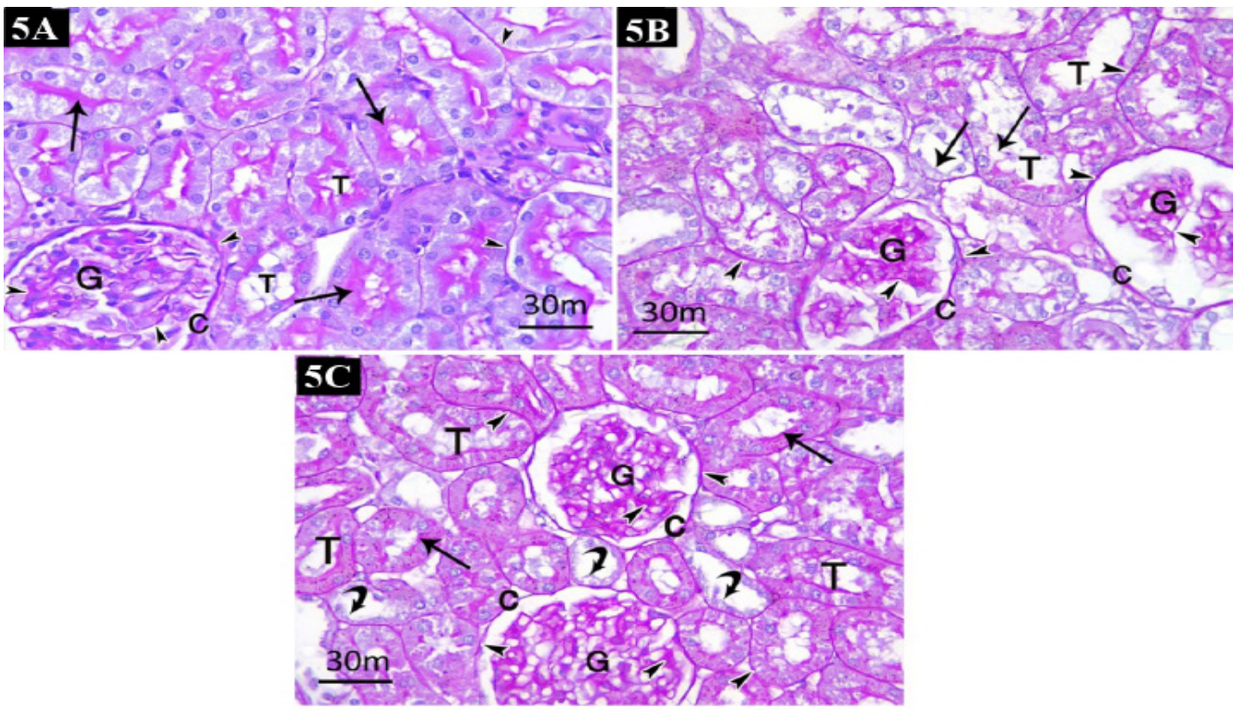


**Fig. 5:** PAS-stained sections. (A) Control group showing positive reaction at the brush borders of the renal tubules (arrow) and the basement membranes (arrow head) of the renal tubules (T), the renal corpuscles (C), and the glomerular capillaries (G). (B) ESWL group showing areas of lost reaction (arrow) in the brush borders of some renal tubules (T). Positive reaction (arrow head) is noticed in the basement membrane of the tubules, the renal corpuscle (C) and glomerular capillaries (G). (C) ESWL treated with medical ozone group showing positive reaction at the brush borders (arrow) of most renal tubules (T), and the basement membranes (arrow head) of the renal tubules, Bowmen's capsule (C) and glomerular capillaries (G). Areas of loss of reaction (curved arrow) are still detected in some tubules. (PAS x400)

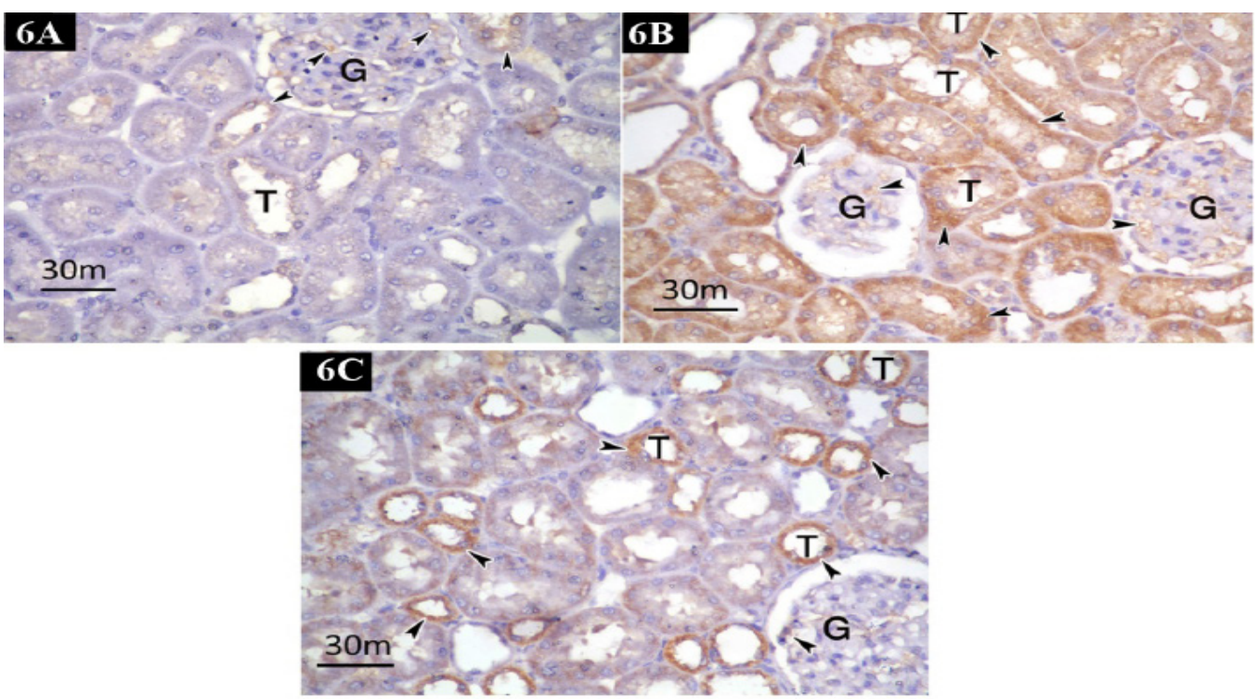


**Fig. 6:** iNOS immunostained sections. (A) Control group showing faint cytoplasmic reaction (arrow head) in a few tubules (T) and glomerular capillaries (G). (B) ESWL group showing increased cytoplasmic reaction (arrow head) in most of tubular lining cells (T) and in some glomerular capillaries (G). (C) ESWL treated with medical ozone group showing increased cytoplasmic reaction (arrow head) in some of the tubular lining cells (T) and in the glomerular capillaries (G). (iNOS immuneperoxidase x400)

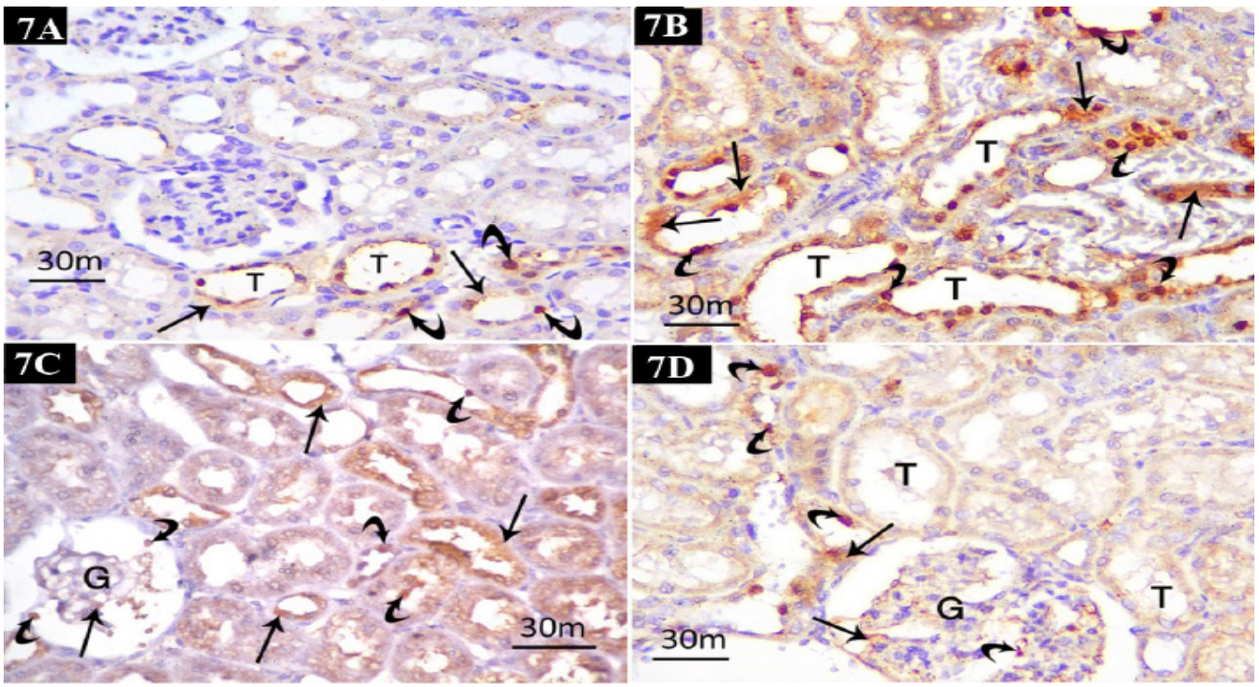


**Fig. 7:** HSP-70 immunostained sections. (A) Control group showing cytoplasmic (arrow) and nuclear (curved arrow) reaction in some renal tubules (T). (B & C) ESWL group showing in (B), increased cytoplasmic (arrow) and nuclear (curved arrow) reactions in the tubular lining cells of many tubules (T). In (C), showing the reaction in the nuclei (curved arrow) and cytoplasm (arrow) of some glomerular capillaries (G). (D) ESWL treated with medical ozone group showing positive reaction both in nuclei (curved arrow) and cytoplasm (arrow) of few tubules (T), and glomerular capillary endothelium (G). (HSP-70 immuneperoxidase x400)

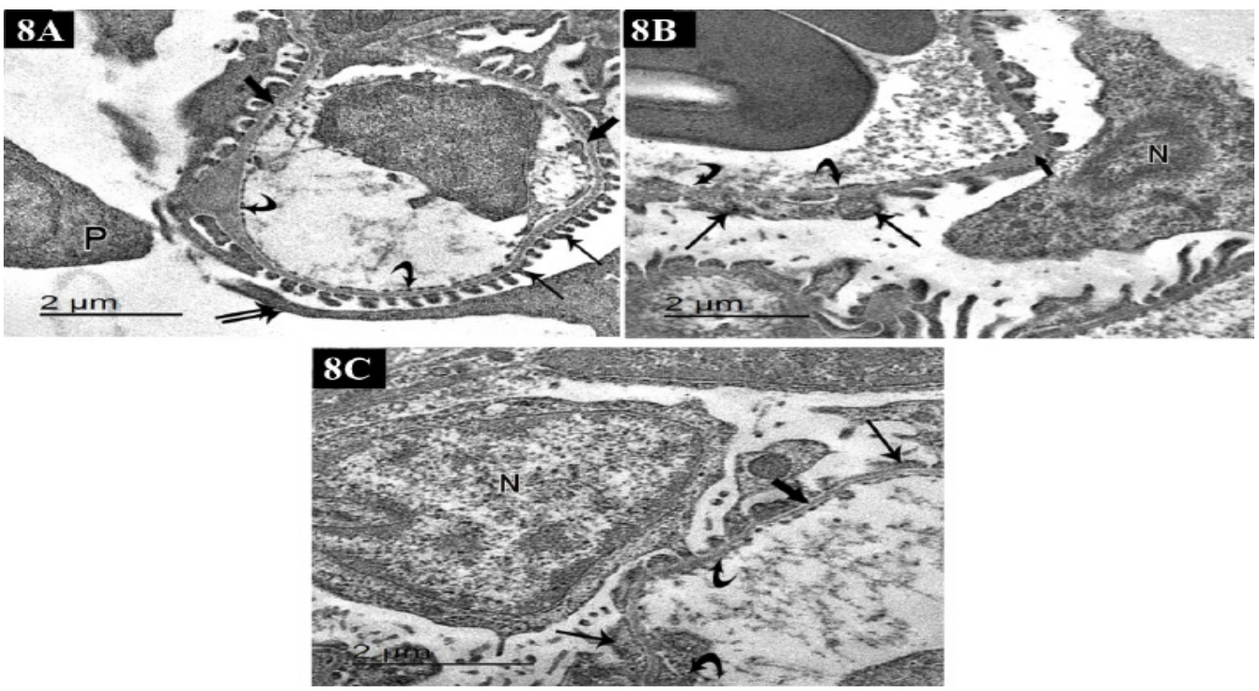


**Fig. 8:** Ultrathin sections of the renal barrier. (A) Control group showing a podocyte (P) with primary processes (double arrow) and interdigitating secondary processes (arrow). The glomerular capillary is lined by thin fenestrated endothelium (curved arrow). The glomerular basement membrane appears thin and uniform (thick arrow). (B) ESWL group showing a podocyte with small heterochromatic nucleus (N) and distorted feet processes (arrow). The endothelium with areas of lost fenestrations (curved arrow) is seen. The glomerular basement membrane is thickened (thick arrow). (C) ESWL treated with medical ozone group showing a podocyte with large pale nucleus (N) and some distorted feet processes (arrow). The glomerular basement membrane appears thin and uniform (thick arrow). A glomerular blood capillary with areas of lost fenestrations (curved arrows) is seen.

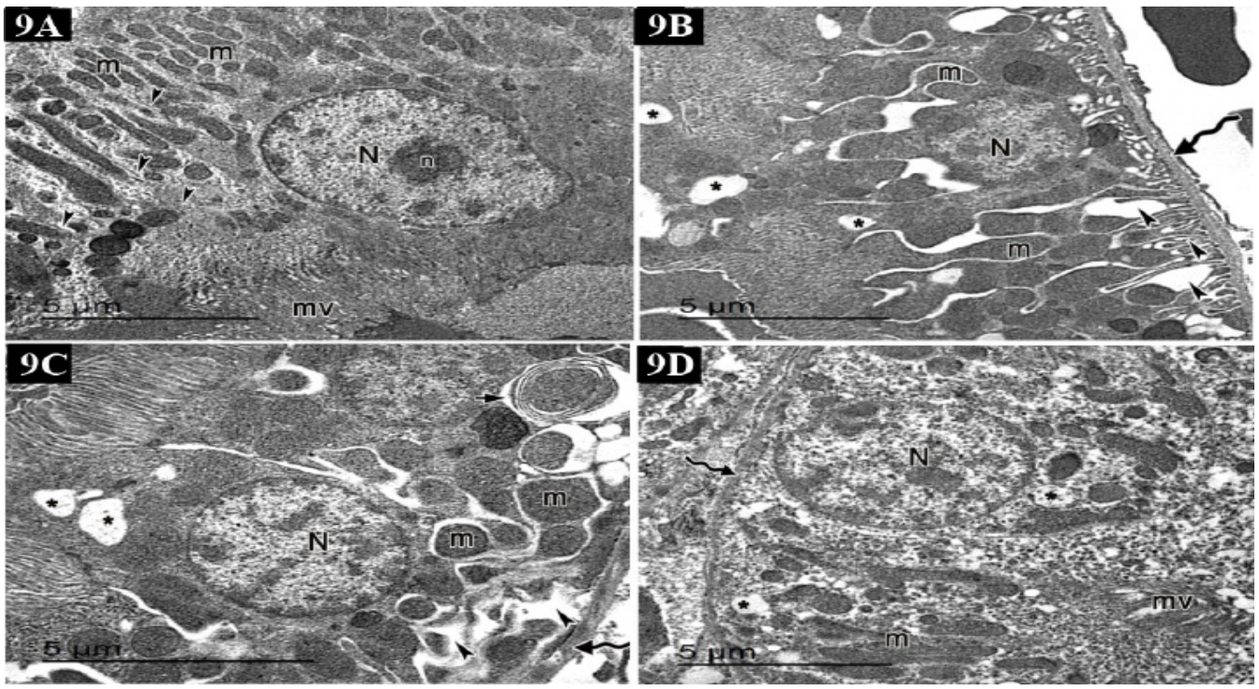


**Fig. 9:** Ultrathin sections of tubular epithelial cells of PCTs. (A) Control group showing the proximal tubular epithelial cell containing pale nucleus (N) with prominent nucleolus (n), and luminal microvilli (mv). Elongated mitochondria (m) are seen lodged within basal infoldings (arrow head). Thin basement membrane (zigzag arrow) is noticed. (B & C) ESWL group showing in (B), a small nucleus (N) with heterochromatic condensation. Apical cytoplasmic vacuoles (asterisk) are noticed. There are irregular and widely separated basal infoldings (arrow heads), and distorted mitochondria (m). Basement membrane is thickened (zigzag arrow). In (C), showing nucleus (N), cytoplasmic vacuolations (asterisk) and swollen distorted mitochondria (m) with masked internal structure. There are irregular basal infoldings (arrow heads). Basement membrane is observed (zigzag arrow). An autophagosome (short arrow) is seen. (D) ESWL treated with medical ozone group showing rounded pale nucleus (N), elongated mitochondria (m) appeared lodged within basal infoldings and apical microvilli (mv). The basement membrane is thin and uniform (zigzag arrow). Cytoplasmic vaculations (asterisks) are seen.

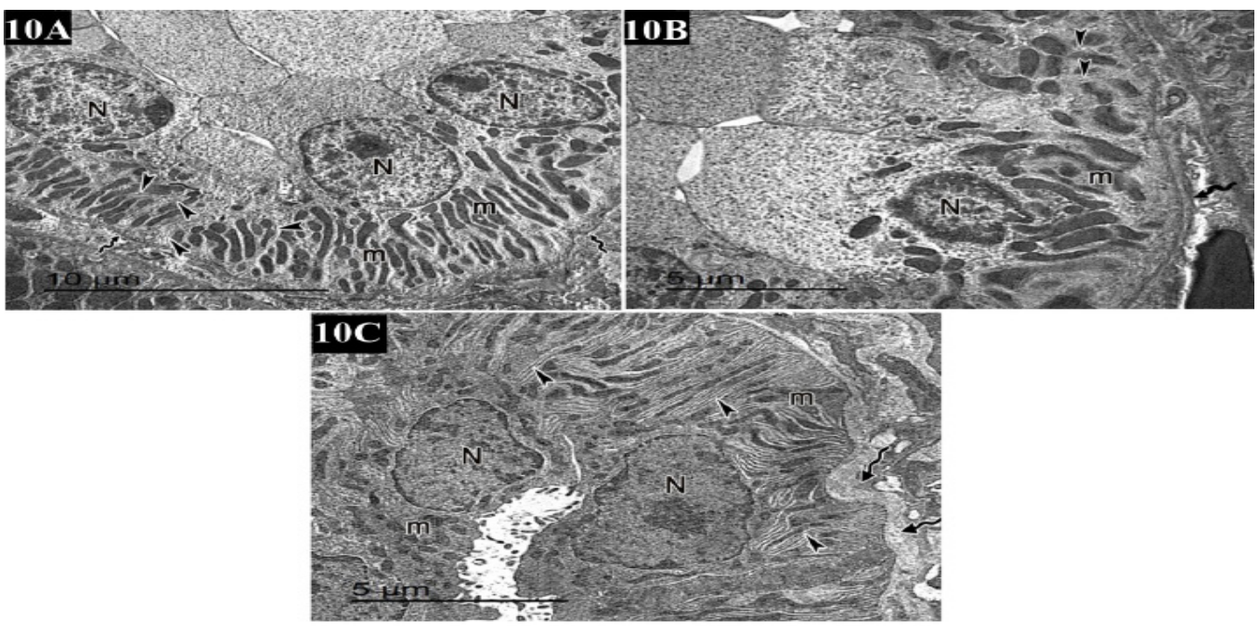


**Fig. 10:** Ultrathin sections of tubular epithelial cells of DCTs. (A) Control group showing pale nuclei (N), elongated mitochondria (m) and regular basal infoldings (arrow head). The basement membrane is thin and uniform (zigzag arrow). (B) ESWL group showing small heterochromatic nucleus (N) is observed. Distorted basal infoldings (arrow heads) and irregular mitochondria (m) are seen. The basement membrane is thickened (zigzag arrow). (C) ESWL treated with medical ozone group showing pale nuclei (N). Elongated mitochondria (m) within their basal infoldings (arrow head) are also observed. The basement membrane is thickened (zigzag arrow).

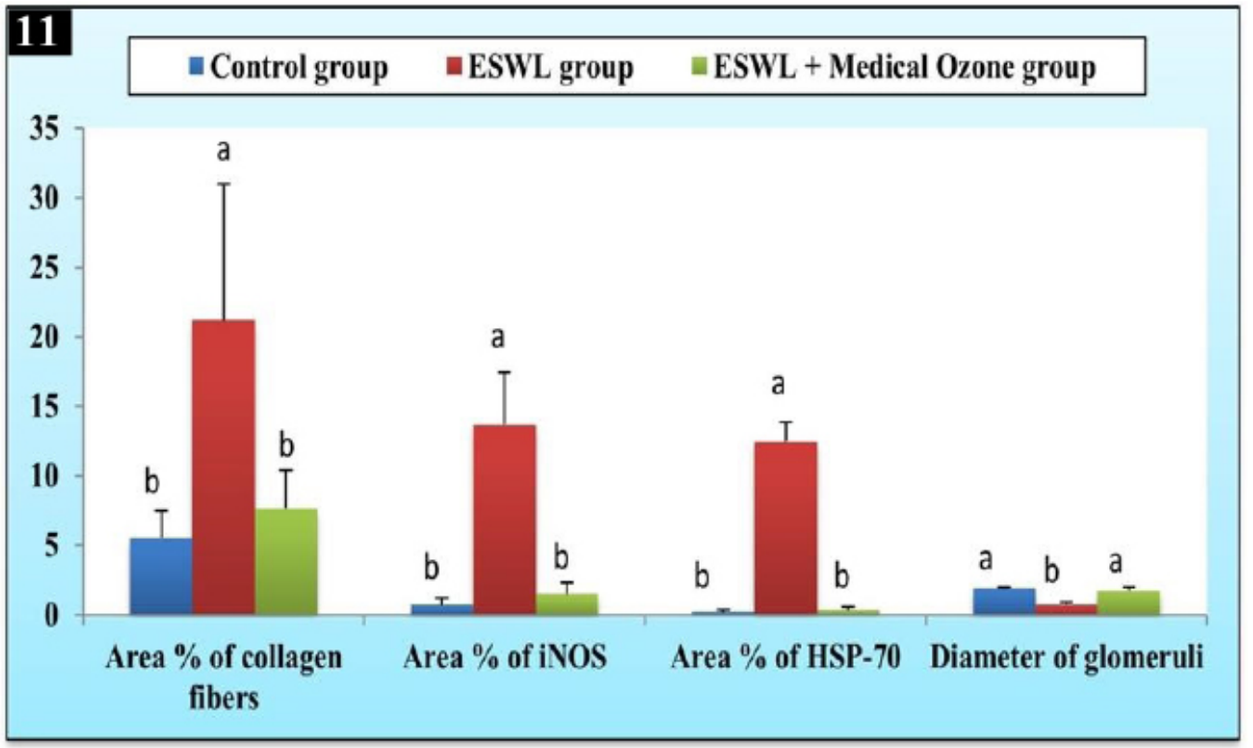


**Fig. 11:** Mean values of area percent of collagen fibers, area percent of iNOS and HSP-70 immunoreaction and diameters of glomeruli in different experimental groups

**Table 1:** Changes in serum urea, serum creatinine, MDA, SOD and GSPx of behavioral tests between different experimental groups.

| Parameters | Control group | ESWL group | ESWL + Medical Ozone group | *P-value* |
|---|---|---|---|---|
| Serum creatinine (mg/dl) | $0.23 \pm 0.01^{b}$ | $0.36 \pm 0.015^{a}$ | $0.24 \pm 0.01^{b}$ | < 0.0001** |
| Serum urea (mg/dl) | $46.00 \pm 3.46^{b}$ | $64.00 \pm 5.57^{a}$ | $51.67 \pm 2.08^{b}$ | < 0.0009** |
| MDA (nmol/g) | $92.17 \pm 5.58^{b}$ | $126.67 \pm 10.69^{a}$ | $98.40 \pm 3.93^{ab}$ | 0.008** |
| SOD (U/gm) | $30.83 \pm 3.33^{b}$ | $16.1 \pm 1.05^{c}$ | $23.97 \pm 3.05^{a}$ | 0.002** |
| GPx (U/gm) | $24.5 \pm 3.5^{a}$ | $11.43 \pm 0.9^{b}$ | $21.1 \pm 0.66^{a}$ | < 0.0001** |

* : Significant ($p$<0.05).
**: Highly significant difference ($p$<0.01).
[ab] Means within the same column carrying different superscripts are significantly different at $p < 0.05$ based on Tukey's Kramer HD test.
S.D.: standard deviation.
Values are expressed as mean (X) ± standard deviation (SD).

**Table 2:** Mean values (± SD) of area percent of collagen fibers, area percent of iNOS and HSP-70 immunoreaction and diameters of glomeruli between different experimental groups.

| Parameters | Control group | ESWL group | ESWL + Medical Ozone group | *P-value* |
|---|---|---|---|---|
| Area % of collagen fibers | $5.49 \pm 1.99^{b}$ | $21.20 \pm 9.75^{a}$ | $7.61 \pm 2.76^{b}$ | 0.001** |
| Area % of iNOS | $0.70 \pm 0.49^{b}$ | $13.67 \pm 3.78^{a}$ | $1.49 \pm 0.85^{b}$ | < 0.0001** |
| Area % of HSP-70 | $0.20 \pm 0.17^{b}$ | $12.43 \pm 1.39^{a}$ | $0.32 \pm 0.28^{b}$ | < 0.0001** |
| Diameter of glomeruli | $1.88 \pm 0.13^{a}$ | $0.75 \pm 0.19^{b}$ | $1.76 \pm 0.20^{a}$ | < 0.0001** |

**: Highly significant difference ($p$<0.01).
[ab]Means within the same column carrying different superscripts are significantly different at $p < 0.05$ based on Tukey's Kramer HD test.
S.D.: standard deviation.
Values are expressed as mean (X) ± standard deviation (SD).

## DISCUSSION

Acute kidney injury (AKI) is a serious clinical illness affecting public health internationally with high death rate, and yet there is no clinically effective treatment. Medical costs are considerable because the majority of operations include supportive care or dialysis[29]. The goal of this study was to shed light on the potential alterations in the renal cortex of adult male albino rats following ESWL exposure, and investigate the ameliorative effect of medical ozone.

In the present study, 2000 shocks with a power level 90-100% at a rate of 60 shock waves per minute were used. It is preferred to use an average of 700 to 3000 shocks of varied voltage to dissolve kidney and ureteral stones. No pathologic changes were reported after administering 500 SWs to animal models[30].

Measurement of serum urea and creatinine in the ESWL group revealed a highly significant increase in their levels compared to the control group. Mohammadi *et al*,[31] explained the previous finding by the reduced GFR.

The ESWL group showed a highly significant reduction in the SOD mean values which was attributed by Li *et al*,[32] to the oxidative stress brought on by IRI. Also, the levels of glutathione peroxidase (GPx); another H2O2 scavenger, were significantly decreased. Costa *et al*, and Gibb *et al*,[33,34] reported that several IRI-induced acute injuries result in a decrease in GPx due to oxidative stress and ROS generation.

In the current work, the statistical analysis of MDA mean values sets up an evidence of cell death by revealing a highly significant rise in the ESWL group in comparison to the other groups. Demir Çaltekin *et al*. declared an increase in MDA levels following ovarian IRI. MDA plays a significant role in AKI and contributes to cell death[35]. As a result of MDA activity distortion, cell membrane permeability and fluidity are compromised. Additionally, it results in cell separation and breakdown of intra-cytoplasmic organelle material[36].

The cells lining the renal tubules revealed vacuolar degeneration and dark nuclei in the ESWL group. Ultrastructural examination exhibited small heterochromatic nuclei, numerous cytoplasmic vacuoles, irregular basal infoldings and swollen mitochondria with masked internal structure. According to Kar *et al*,[37] IRI-induced tubular atrophy is a result of reactive oxygen species generation that attack cell membranes, and cause lipid peroxidation. Proximal convoluted tubules (PCTs) are the main target cells of acute IRI depending on the degree of injury[38]. Due to the actions of neutrophils and damaged mitochondria, free radicals caused degenerative changes in the tubular epithelial cells. ROS retention causes breakage of DNA and deterioration of the cell and organelle membranes resulting in cell death through necrosis, apoptosis and autophagy[39].

In the same context, Fawzy *et al*,[40] clarified that nuclear factor kappa B (NF-kB) controls inflammation and apoptosis during IRI, and the hypoxia that takes place during this process blocks the oxygen receptor and stimulates NF-kB. Other studies attributed apoptosis to an excess of ROS production, up regulation of Bax expression and down regulation of Bcl-2 expression[41].

Increased cytosolic calcium ions activate the mitochondrial permeability transition pore; a non-specific channel that contributes to swollen mitochondria and result in loss of the internal mitochondrial membrane impermeability to solutes (mPTP). This process results in mitochondrial swelling which leads to mitochondrial malfunction and activation of the apoptotic pathway[42].

The cytoplasmic vacuoles and autophagosomes observed in the current study were attributed by Doherty *et al*,[43] to excessive autophagy that results in excessive destruction of vital proteins and organelles causing autophagic cell death. Reperfusion can also induce autophagy as it prevents the injured mitochondria from producing harmful chemicals which is one protective function of autophagy[44].

In addition, the ESWL group revealed shrinkage of glomeruli with wide bowman's space that was statistically confirmed by a highly significant decline in the glomerular diameter in comparison to the control. Roshankhah *et al*,[45] found that renal I/R considerably reduced the mean glomerulus diameter. Also, there was congestion of some glomeruli and peri-tubular capillaries in the ESWL group. According to Cai *et al*,[46], vascular permeability changes are directly associated to AKI, and the micro-vascular hypo-perfusion, edema, hypoxia, and inflammation are caused by capillary hyper-permeability to proteins exacerbating tissue damage and dysfunction.

The blood renal barrier (BRB) from sections in the ESWL group exhibited glomerular capillary endothelial damage, thickened glomerular basement membrane and deformed podocytes feet processes. Similar results were obtained by Chen *et al*,[47] who added that renal ischemia at 30 minutes after reperfusion lowered the expression of the functional proteins nephrin and synaptopodin.

The renal cortex interstitium in the ESWL group revealed cellular infiltration. In the initial phases of IRI, neutrophils migrate and adhere to the site of damaged tissues releasing (IL-7). Moreover, pro-inflammatory cytokines including tumor necrosis factor alpha (TNF) are released from macrophages causing cells to go into apoptosis[48].

Some renal tubules in the ESWL group showed focal loss of PAS reaction in their brush borders which was in line with Huang *et al*,[49] who reported that the glycocalyx damage is caused by AKI-induced oxidative stress. During oxidative stress, the uncoupled endothelial nitric oxide synthase (eNOS) induces endothelial cell dysfunction, activation and recruitment of leukocytes and results in denudation of the glycocalyx[50].

ESWL group sections showed capsular thickening with prominent perivascular and interstitial fibrosis which was confirmed statistically as the area% of collagen fibers was significantly higher in the ESWL group compared to the control. In agreement, Demir *et al*,[30] showed extensive perivascular and ureteral fibrosis after application of high dose and high energy ESWL. In previous researches using a rat model, shock waves caused tubular injury, interstitial infiltration, and tubulo-interstitial fibrosis. Renal fibrosis is mostly attributed to the epithelial-mesenchymal transition (EMT) brought on by oxidative stress[51,52].

Regarding immune localization of iNOS in the renal cortex of the ESWL group, there was a significant increase in its area% compared to the control. Similar results were obtained by Gao *et al*, and Roshankhah *et al*,[53,45]. This finding was explained by enhancing synthesis of inducible nitric oxide synthase (iNOS) as a result of elevated levels of TNF-α, IFN-γ and IL-1β[54]. Following renal IR, the expression of iNOS increases in tubules augmenting NO production while the expression of eNOS is inhibited reducing NO production from endothelium and as a result vasoconstriction occurs[55].

The ESWL group also revealed a significant increase in area% of HSP-70 immune-reactivity as compared to the control. Golmohammadi *et al*,[56] reported that IR markedly elevated the expression of caspase-3 and HSP-70. Ullah *et al*,[57] added that cisplatin-induced AKI up-regulates the expression of HSP-70 and HSP-90. HSP-70 expression was up-regulated in the renal cortex during AKI in order to clear out mis-folded proteins caused by oxidative damage and to guarantee the correct shape of newly generated proteins[58]. ROS encourages the creation of HSP-70 to shield enzymes and other cell components from the damaging effects of ROS[59].

In the present study, administration of medical ozone was proved to improve the renal cortex. Functionally, there was non-significant difference between the medical ozone and the control groups regarding the levels of serum creatinine and urea. The histological structure was nearly similar to the control apart from some congested capillaries, few cytoplasmic vacuoles and distorted feet processes.

Wang *et al*,[60] explained the previous findings as O3 delivery can affect particular systems to enhance cell survival and proliferation by preventing the apoptotic processes. Caspases 1-3-9, hypoxia-inducible factor (HIF), tumor necrosis factor-a (TNF-), Bcl-2-associated X protein (Bax), poly (ADP-ribose) polymerase 1 (PARP-1) and p53 gene expression are all specifically down-regulated by O3. Zeng *et al*,[61] added that in patients who received ozonated autohemotherapy (OAHT) treatment, ozone modulated local neutrophil accumulation, IL-6, TNF-, IL-17a and IL-23 expression in skin disorders, and increased the total local antioxidant capacity.

According to Singh *et al*.[62], after ozone is administered, it instantly dissolves in plasma and interacts with macromolecular glycoproteins. These substances are oxidized to form $H_2O_2$ which may alter cellular metabolism to promote tissue regeneration, activate the innate immune system and support cell survival in response to IRI. Han *et al*,[63] reported that ozone oxidative pre-conditioning could reduce the inflammatory reaction and oxidative stress injury in renal allograft. Similarly, O3 preconditioning was reported to have a protective effect on myocardial IRI by up-regulation of HIF-1α; a key mediator of cellular homeostasis in response to hypoxia, which plays an important role by reducing mitochondrial dysfunction[64].

By boosting the oxidative carboxylation of pyruvate and promoting the synthesis of adenosine triphosphate (ATP), medical ozone activates Kreb's cycle in mitochondria. It also causes a significant reduction of nicotinamide adenine dinucleotide (NADH) and an increase of the coenzyme A levels to fuel the Kreb's cycle and oxidize cytochrome C[65].

Cai *et al*,[66] described how oxidative stress-induced cell injury could increase MDA. A considerable drop in MDA following ozone therapy showed that ozone significantly reduced the mitochondrial oxidative damage brought on by I/R injury[67].

In the current work, the medical ozone group displayed a reduction in the amount of collagen fibers surrounding the renal corpuscles, renal tubules and blood vessels. There was a non-significant difference in the area % of collagen fibers in comparison to the control group. This was consistent with Wang *et al*,[68] who described how ozone may have a novel therapeutic function in the treatment of ischemic renal fibrosis by altering the TGF-1/Smad7 pathway.

Regarding iNOS immunoreaction in the medical ozone group, it was non-significant compared to the control group. Nitric oxide (NO) overproduction can be prevented by using medical ozone. Medical ozone inhibits iNOS which produces NO through NF-B signaling[69,70]. Previous studies demonstrated the capacity of ozone to increase NO levels in some organs including the liver, heart, muscles, kidney and testis, as well as to activate and up-regulate the genes connected to NOS[71].

On the other hand, non significant difference in the area % of HSP-70 immune reactivity was found between the medical ozone and the control groups. In agreement Salama and Elmalt,[72] stated that pre-treatment and post-treatment with other antioxidants significantly reduced renal TNF-α, TLR4 and HSP-70 contents.

Ozone has been shown in studies to activate the body defenses against oxidative stress and to promote the production of nuclear factor erythroid 2-related factor 2 (Nrf2)/electrophile-responsive element (EpRE). Nrf2 was reported to boost the action of the antioxidant enzymes and controls the induced expression of antioxidants such as superoxide dismutase, glutathione peroxidase and catalase[73,74].

In the same context, assessment of the anti-oxidant enzyme profile in the present work revealed a non-

significant difference in tissue SOD and GPx in the medical ozone group when compared to the control. Similar results were obtained by Izadi *et al*,[75]. Akman *et al*,[76] discovered that medical ozone therapy raised the enzyme activity values of the antioxidant enzymes (SOD, GPx) in case of spinal cord ischemia in rats.

## CONCLUSION

In conclusion, the current study proved the negative impact of ESWL on adult rat renal cortex, both structurally and functionally. The ESWL caused significantly high levels of serum creatinine and urea and tissue MDA, and decreased SOD and GPx levels. There were shrinkage of glomeruli, distorted feet processes and thick basement membrane. Tubules were distorted with cytoplasmic vacuoles, congested peritubular capillaries and cellular infiltration in the interstitium. The area% of collagen fibers and iNOS and HSP-70 immunoreactivity increased while the glomerular diameter decreased. Medical ozone caused marked improvement, both structurally and functionally. Our findings supported the need to enhance patient care in order to lessen the immediate renal damage brought on by ESWL. Therefore, ozone therapy is suggested as a potential agent to prompt the improvement of kidney structure and function through enhancing autophagy and antioxidant and anti-inflammatory properties. Further studies should be applied to delineate the effectiveness of medical ozone on long run and to adjust the most appropriate mode of administration for management of acute kidney injury.

## CONFLICT OF INTERESTS

There are no conflicts of interest.


1. Skowron B, Baranowska A, Kaszuba-Zwoińska J, Więcek G, *et al*. Experimental model for acute kidney injury caused by uropathogenic Escherichia coli. Postępy Higieny i Medycyny Doświadczalnej. 2017; 71: 520-529. doi: 10.5604/01.3001.0010.3833
2. Finlay S and Jones MC. Acute kidney injury. Medicine. 2017; 45(3): 173-176. doi: 10.1016/j.mpmed.2016.12.010
3. Parameswaran P and Devarajan P. Cellular and Molecular Mechanisms of Acute Kidney Injury. Critical Care Nephrology. 2019; 3rd ed., p.p. 1194-1204. Elsevier. Philadelphia
4. Salama A and Elmalt H. Aescin ameliorate acute kidney injury induced by potassium dichromate in rat: involvement of TLR 4/TNF-α pathway. Egyptian Journal of Chemistry, 2021; 64(4): 67-74.
5. Turgut F, Awad A and Abdelrahman E. acute kidney injury: medical causes and pathogenesis. Journal of clinical medicine. 2023; 12(1): 375-385.
6. Makris K and Spanou L. Acute kidney injury: definition, pathophysiology and clinical phenotypes. The Clinical Biochemist Reviews. 2016 May; 37(2): 85-98.
7. Türk C, Petřík A, Sarica K, Seitz C, *et al*. EAU guidelines on interventional treatment for urolithiasis. European urology. 2016 Mar 1; 69(3):475-482. doi: 10.1016/j.eururo.2015.07.041
8. Dzięgała M, Krajewski W, Kołodziej A, Dembowski J, *et al*. Evaluation and physiopathology of minor transient shock wave lithotripsy–induced renal injury based on urinary biomarkers levels. Central European journal of urology. 2018; 71(2): 214-220. doi: 10.5173/ceju.2018.1629
9. Mercimek MN, Bostancı Y, Özden E, *et al*. Protective effects of oral sirolimus therapy against ESWL-induced kidney tissue damage in rats. Journal of Urological Surgery. 2019 Sep 1; 6(3): 190-195. doi: 10.4274/jus.galenos.galenos.2019.2492
10. Oksidatif SO. The efficacy of N-acetylcysteine against renal oxidative stress after extracorporeal shock wave treatment: An experimental rat model. Journal of Urological Surgery. 2020; 7(1): 8-15. doi: 10.4274/jus.galenos.2019.2941
11. Smith NL, Wilson AL, Gandhi J, Vatsia S, *et al*. Ozone therapy: an overview of pharmacodynamics, current research, and clinical utility. Medical gas research. 2017 Jul; 7(3): 212-219. doi: 10.4103/2045-9912.215752
12. Ozturk O, Eroglu HA, Ustebay S, and Kuzucu M. An experimental study on the preventive effects of N-acetyl cysteine and ozone treatment against contrast-induced nephropathy. Acta cirurgica brasileira. 2018; 33(6): 508-517. doi: 10.1590/s0102-865020180060000005
13. Di Mauro R, Cantarella G, Bernardini R, Di Rosa M. *et al*. The biochemical and pharmacological properties of ozone: the smell of protection in acute and chronic diseases. International journal of molecular sciences. 2019;20(3): 634-647.
14. Colakerol A, Suzan S, Temiz MZ, Gonultas S, *et al*. Tissue neutrophil elastase contributes to extracorporeal shock wave lithotripsy-induced kidney damage and the neutrophil elastase inhibitor, sivelestat, attenuates kidney damage with gratifying immunohistopathological and biochemical findings: an experimental study. Urolithiasis. 2021 Feb; 50(1): 103-112. doi: 10.1007/s00240-021-01287-x
15. Kızılay Z, Kahraman Çetin N, Aksel M, Abas Bİ *et al*. Ozone partially decreases axonal and myelin damage in an experimental sciatic nerve injury model. Journal of Investigative Surgery. 2019 Jan 2; 32(1): 8-17. doi: 10.1080/08941939.2017.1369606
16. Handa RK, Territo PR, Blomgren PM, and Persohn SA. Development of a novel magnetic resonance imaging acquisition and analysis workflow for the quantification of shock wave lithotripsy-induced renal hemorrhagic injury. Urolithiasis. 2017 Oct; 45(5): 507-513. doi: 10.1007/s00240-016-0959-5

17. Uğuz S, Demirer Z, Uysal B, Alp BF, *et al*. Medical ozone therapy reduces shock wave therapy-induced renal injury. Renal failure. 2016; 38(6): 974-981.

18. Wen L, Gao Q, and Wah Ma C, *et al*. Effect of polysaccharides from Tremella fuciformis on UV-induced photoaging. Journal of Functional Foods. 2016 Jul 2; 20: 974-981. doi: 10.3109/0886022X.2016.1172941

19. Arkill K, Neal C, Mantell J, *et al*. 3D reconstruction of the glycocalyx structure in mammalian capillaries using electron tomography. Microcirculation. 2012; 19(4):343-351.

20. Ali AA, Abd el-latif DM, Gad AM, *et al*. nephrotoxicity and hepatotoxicity induced by chronic aluminum exposure in rats: impact of nutrients combination versus social isolation and protein malnutrition. The Arab journal laboratory medicine. 2018; 43(2): 195-213.

21. Nishikimi M, Rao NA, and Yagi K. The occurrence of superoxide anion in the reaction of reduced phenazine methosulfate and molecular oxygen. Biochemical and biophysical research communications. 1972 Jan 31; 46(2): 849-854. doi: 10.1016/S0006-291X(72)80218-3

22. Paglia DE, and Valentine WN. Studies on the quantitative and qualitative characterization of erythrocyte glutathione peroxidase. The Journal of laboratory and clinical medicine. 1967 Jul 1; 70(1): 158-169. doi: 10.5555/uri:pii:0022214367900765

23. Ohkawa H, Ohishi N, and Yagi K. Assay for lipid peroxides in animal tissues by thiobarbituric acid reaction. Analytical biochemistry. 1979 Jun 1; 95(2): 351-358. doi: 10.1016/0003-2697(79)90738-3

24. Suvarna KS, Layton C, and Bancroft JD. Bancroft's Theory and Practice of Histological Techniques E-Book. Elsevier health sciences; 2018. 8th ed., p.p. 337-395. Elsevier, China.

25. Abo-Elmaaty A, Behairy A, El-Naseery NI. & Abdel-Daim M. The protective efficacy of vitamin E and cod liver oil against cisplatin-induced acute kidney injury in rats. Environmental Science and Pollution Research, 2020; 27(35): 12-26

26. Chung J, Park B, Kim J. *et al*. Impact of repeated extracorporeal shock wave lithotripsy on prepubertal rat kidney. Urolithiasis, 2018; 46(6): 549-558.

27. Singh D. Principle and Technique in Histology, Microscopy and Photography. CBS Publishers and Distributers; 2003. 1st ed., p.p. 669-679., New Delhy and Bangalore, India.

28. Lee S. and Lee D. What is the proper way to apply the multiple comparison test?. Korean journal of anesthesiology. 2018; 71(5): 353.

29. Mehta RL, Cerdá J, Burdmann EA, Tonelli M, *et al*. International Society of Nephrology's 0by25 initiative for acute kidney injury (zero preventable deaths by 2025): a human rights case for nephrology. The Lancet. 2015 Jun 27; 385(9987): 2616-2643. doi: 10.1016/S0140-6736(15)60126-X

30. Demir A, Türker P, Bozkurt SU, and İlker YN. The histomorphological findings of kidneys after application of high dose and high-energy shock wave lithotripsy. Central European journal of urology. 2015; 68(1): 72-78. doi: 10.5173%2Fceju.2015.01.480

31. Mohammadi M, Najafi H, Yarijani ZM, Vaezi G, *et al*. Protective effect of piperine in ischemia-reperfusion induced acute kidney injury through inhibition of inflammation and oxidative stress. Journal of Traditional and Complementary Medicine. 2020 Nov 1; 10(6): 570-576. doi: 10.1016/j.jtcme.2019.07.002

32. Li J, Li L, Wang S, and Zhang C, *et al*. Resveratrol alleviates inflammatory responses and oxidative stress in rat kidney ischemia-reperfusion injury and H2O2-induced NRK-52E cells via the Nrf2/TLR4/NF-κB pathway. Cellular Physiology and Biochemistry. 2018; 45(4): 1677-1689. doi: 10.1159/000487735

33. Costa CC, Pereira NG, Machado AL, Dórea MA, *et al*. Splenic ischemic preconditioning attenuates oxidative stress induced by hepatic ischemia-reperfusion in rats. Acta Cirúrgica Brasileira. 2019 Sep; 34(7): 1-7. doi: 10.1590/s0102-865020190070000007

34. Gibb Z, Blanco-Prieto O, and Bucci D. The role of endogenous antioxidants in male animal fertility. Research in Veterinary Science. 2021 May 1; 136: 495-502. doi: 10.1016/j.rvsc.2021.03.024

35. Demir Çaltekin M, Özkut M, Çaltekin İ, Kaymak E. *et al*. The protective effect of JZL184 on ovarian ischemia reperfusion injury and ovarian reserve in rats. Journal of Obstetrics and Gynaecology Research, 2021; 47(8): 2692-2704.

36. Ben-Mahdi MH, Dang PM, Gougerot-Pocidalo MA, *et al*. Xanthine oxidase-derived ROS display a biphasic effect on endothelial cells adhesion and FAK phosphorylation. Oxidative Medicine and Cellular Longevity. 2016 Jan 1; 1-9. doi: 10.1155/2016/9346242

37. Kar F, Hacioglu C, Senturk H, Donmez DB, *et al*. The role of oxidative stress, renal inflammation, and apoptosis in post ischemic reperfusion injury of kidney tissue: the protective effect of dose-dependent boric acid administration. Biological trace element research. 2020 May; 195(1): 150-158. doi: 10.1007/s12011-019-01824-1

38. Chevalier RL. The proximal tubule is the primary target of injury and progression of kidney disease: role of the glomerulotubular junction. American Journal of Physiology-Renal Physiology. 2016 Jul 1; 311(1): 145-161. doi: 10.1152/ajprenal.00164.2016

39. Elsawy H Alzahrani A M, Alfwuaires M, Abdel-Moneim A M, & Khalil M. Nephroprotective effect of naringin in methotrexate induced renal toxicity in male rats. Biomedicine & Pharmacotherapy, 2021;143:1-15.

40. Fawzy MA, Maher SA, El-Rehany MA, Welson NN, *et al*. Vincamine Modulates the Effect of Pantoprazole in Renal Ischemia/Reperfusion Injury by Attenuating MAPK and Apoptosis Signaling Pathways. Molecules. 2022 Feb 18; 27(4): 1383-1399. doi: 10.3390/molecules27041383

41. Fathy M, Awale S, and Nikaido T. Phosphorylated akt protein at ser473 enables hela cells to tolerate nutrient-deprived conditions. Asian Pacific journal of cancer prevention. 2017; 18(12): 3255–3260. doi: 10.22034/APJCP.2017.18.12.3255

42. Ma Z, Xin Z, Di W, Yan X, *et al*. Melatonin and mitochondrial function during ischemia/reperfusion injury. Cellular and molecular life sciences. 2017 Nov; 74(21): 3989-3998. doi: 10.1007/s00018-017-2618-6

43. Doherty J, and Baehrecke EH. Life, death and autophagy. Nature cell biology. 2018 Oct; 20(10): 1110-1117. doi: 10.1038/s41556-018-0201-5

44. Jackson CW, Escobar I, Xu J, and Perez-Pinzon MA. Effects of ischemic preconditioning on mitochondrial and metabolic neruoprotection: 5'adenosine monophosphate-activated protein kinase and sirtuins. Brain circulation. 2018 Apr; 4(2): 54-61. doi: 10.4103/bc.bc_7_18

45. Roshankhah S, Jalili C, and Salahshoor MR. Protective effects of Petroselinum crispum on ischemia/reperfusion-induced acute kidney injury in rats. Physiology and Pharmacology. 2019 Jul 10; 23(2): 129-139. doi: 20.1001.1.24765236.2019.23.2.3.5

46. Cai A, Chatziantoniou C, and Calmont A. Vascular permeability: regulation pathways and role in kidney diseases. Nephron. 2021; 145(3): 297-310. doi: 10.1159/000514314

47. Chen Y, Lin L, Tao X, Song Y, *et al*. The role of podocyte damage in the etiology of ischemia-reperfusion acute kidney injury and post-injury fibrosis. BMC nephrology. 2019 Dec; 20(1): 1-11. doi: 0.1186/s12882-019-1298-x

48. Kurzhagen JT, Dellepiane S, Cantaluppi V, and Rabb H. AKI: an increasingly recognized risk factor for CKD development and progression. Journal of Nephrology. 2020 Dec; 33(6): 1171-1187. doi: 10.1007/s40620-020-00793-2

49. Huang ZW, Shi Y, Zhai YY, Du CC, *et al*. Hyaluronic acid coated bilirubin nanoparticles attenuate ischemia reperfusion-induced acute kidney injury. Journal of Controlled Release. 2021 Jun 10; 334: 275-289. doi: 10.1016/j.jconrel.2021.04.033

50. Gómez H, and Kellum JA. Sepsis-induced acute kidney injury. Critical care nephrology. 2019 Jan 1; 524-533. doi: 10.1016/B978-0-323-44942-7.00090-X

51. Carew RM, Wang B, and Kantharidis P. The role of EMT in renal fibrosis. Cell and tissue research. 2012 Jan; 347(1): 103-116. doi: 10.1007/s00441-011-1227-1

52. Song Y, Tao Q, Yu L, Li L. *et al*. Activation of autophagy contributes to the reno-protective effect of post conditioning on acute kidney injury and renal fibrosis. Biochemical and biophysical research communications, 2018;504(4): 641-646

53. Gao D, Jing S, Zhang Q, and Wu G. Pterostilbene protects against acute renal ischemia reperfusion injury and inhibits oxidative stress, inducible nitric oxide synthase expression and inflammation in rats via the Toll like receptor 4/nuclear factor κB signaling pathway. Experimental and Therapeutic Medicine. 2018 Jan 1; 15(1): 1029-1035. doi: 10.3892/etm.2017.5479

54. Saini R, and Singh S. Inducible nitric oxide synthase: an asset to neutrophils. Journal of Leukocyte Biology. 2019 Jan; 105(1): 49-61. doi: 10.1002/JLB.4RU0418-161R

55. Xu N, Jiang S, Persson PB, Persson EA, *et al*. Reactive oxygen species in renal vascular function. Acta Physiologica. 2020 Aug; 229(4): 1-15. doi: 10.1111/apha.13477

56. Golmohammadi MG, Banaei S, Nejati K, and Chinifroush-Asl MM. Vitamin D3 and erythropoietin protect against renal ischemia-reperfusion injury via heat shock protein 70 and microRNA-21 expression. Scientific Reports. 2020 Dec 1; 10(1): 1-9. doi: 10.1038/s41598-020-78045-3

57. Ullah M, Liu DD, Rai S, and Concepcion W, *et al*. HSP70-mediated NLRP3 inflammasome suppression underlies reversal of acute kidney injury following extracellular vesicle and focused ultrasound combination therapy. International journal of molecular sciences. 2020 Jun 8; 21(11): 4085-4098. doi: 10.3390/ijms21114085

58. Akin AT, Unsal M, Ceylan T, Kaymak E, *et al*. Melatonin mitigates cisplatin-induced acute kidney injury through regulation of the heat shock proteins expressions. Research square. 2021; 1-19. doi:10.21203/rs.3.rs-703570/v1

59. Kurashova NA, Madaeva IM, and Kolesnikova LI. Expression of HSP70 heat-shock proteins under oxidative Stress. Advances in Gerontology. 2020 Jan; 10(1): 20-25. doi: 10.1134/S2079057020010099

60. Wang L, Chen Z, Liu Y, Du Y, and Liu X. Ozone oxidative postconditioning inhibits oxidative stress and apoptosis in renal ischemia and reperfusion injury through inhibition of MAPK signaling pathway. Drug design, development and therapy. 2018; 12: 1293–1301. doi: 10.2147/DDDT.S164927

61. Zeng J, Tang Z, Zhang Y, and Tong X, *et al*. Ozonated autohemotherapy elevates PPAR-γ expression in CD4+ T cells and serum HDL-C levels, a potential immunomodulatory mechanism for treatment of psoriasis. American journal of translational research. 2021; 13(1): 349-359.

62. Singh G, Srivsatava S, Shekhar A, Chaturvedi A, *et al*. Ozone Applications in Dentistry: A Biological Therapy. Onlinegatha. 2020 Dec 27; 36-41.

63. Han Q, Wang Z, Guo Y, Liu X, *et al*. Effect of ozone oxidative preconditioning on inflammation and oxidative stress injury in rat model of renal transplantation. Acta cirurgica brasileira, 2018; 33:238-249.

64. Wang R, Liu F, Huang P, Zhang Y, *et al*. Ozone preconditioning protects rabbit heart against global ischemia-reperfusion injury in *vitro* by up-regulating HIF-1α. Biomedicine and Pharmacotherapy. 2022 Jun 1; 150: 113033- 113033. doi: 10.1016/j.biopha.2022.113033

65. Scassellati C, Galoforo AC, Bonvicini C, and Esposito C, *et al*. Ozone: a natural bioactive molecule with antioxidant property as potential new strategy in aging and in neurodegenerative disorders. Ageing research reviews. 2020 Nov 1; 63: 101138-101138. doi: 10.1016/j.arr.2020.101138

66. Cai HA, Tao X, Zheng LJ, Huang L, *et al*. Ozone alleviates ischemia/reperfusion injury by inhibiting mitochondrion-mediated apoptosis pathway in SH-SY5Y cells. Cell biology international. 2020 Apr; 44(4): 975-984. doi: 10.1002/cbin.11294

67. Eroğlu H, Makav M, Adali Y, and Citil M. Effects of ozone and L-carnitine on kidney MDA, GSH, and GSHPx levels in acetaminophen toxicity. Kafkas Universitesi Veteriner Fakultesi Dergisi. 2020; 26(1): 127-134. doi: 10.9775/kvfd.2019.22456

68. Wang L, Chen H, Liu XH, Chen ZY, *et al*. Ozone oxidative preconditioning inhibits renal fibrosis induced by ischemia and reperfusion injury in rats. Experimental and therapeutic medicine. 2014 Dec 1; 8(6): 1764-1768. doi: 10.3892/etm.2014.2004

69. Mete F, Tarhan H, Celik O, Akarken I, *et al*. Comparison of intraperitoneal and intratesticular ozone therapy for the treatment of testicular ischemia-reperfusion injury in rats. Asian Journal of Andrology. 2017 Jan; 19(1): 43-46. doi: 10.4103/1008-682X.171570

70. 70. Manoto SL, Maepa MJ, and Motaung SK. Medical ozone therapy as a potential treatment modality for regeneration of damaged articular cartilage in osteoarthritis. Saudi journal of biological sciences. 2018 May 1; 25(4): 672-679. doi: 10.1016/j.sjbs.2016.02.002

71. Smith N, Wilson A, Gandhi J, Vatsia S, *et al*. Ozone therapy: an overview of pharmacodynamics, current research, and clinical utility. Medical gas research, 2017,7(3): 212-219.

72. Salama A, and Elmalt H. Aescin ameliorates acute kidney injury induced by potassium dichromate in rat: involvement of TLR 4/TNF-α pathway. Egyptian Journal of Chemistry. 2021 Apr 1; 64(4): 2067-2074. doi: 10.21608/ejchem.2021.57553.3237

73. Fernandez JL, Cepero SS, and Rodríguez ZZ. Ozone Therapy on Rats Submitted To Subtotal Nephrectomy: Role of Interleukin 6 and Antioxidant System. Revista Cubana de Investigaciones Biomédicas. 2019 May 27; 38(1): 1-10.

74. Galiè M, Costanzo M, Nodari A, Boschi F. Mild ozonisation activates antioxidant cell response by the Keap1/Nrf2 dependent pathway. Free Radical Biology and Medicine. 2018 Aug 20; 124: 114-121. doi: 10.1016/j.freeradbiomed.2018.05.093

75. Izadi M, Cegolon L, Javanbakht M, Sarafzadeh A, *et al*. Ozone therapy for the treatment of COVID-19 pneumonia: A scoping review. International Immunopharmacology. 2021 Mar 1; 92: 107307-107315. doi: 10.1016/j.intimp.2020.107307

76. Akman T, Aras A, Şimşek T, Şehitoğlu MH, *et al*. The ameliorative effect of ozone therapy on spinal cord ischemia in rabbits. Annals of Clinical and Analytical Medicine. 2020; 11(3): 221-226. doi: 10.4328/ACAM.6215

**الملخص العربى**

# دراسة هستولوجية وهستوكيميائية مناعية على تأثير الأوزون الطبي على الاصابة الحادة لقشرة الكلى المحدثة بموجات جهاز تفتيت الحصوات في ذكور الجرذان المهق البالغة

**نهاد فهمي مازن، عائشة عبدالمنعم الخضري، سارة علي قنديل، ابتهال زيد حسن**

**قسم الهستولوجيا الطبية وبيولوجيا الخلية، كلية الطب، جامعة الزقازيق، الزقازيق، مصر**

**المقدمة:** الإصابة الحادة في الكلى الناجمة عن ضخ الدم الاقفاري بسبب التعرض لجهاز تفتيت حصوات الكلي بموجات الصدمة خارج الجسم.

**المواد والطرق:**. أربعة وأربعون فأراً بالغاً من جرذان الويستار قسموا إلى مجموعة ضابطة: انقسمت إلى مجموعة ضابطة سلبية (لم تتلق أي معالجة) ومجموعة ضابطة إيجابية (تلقت حقنة داخل الصفاق من مزيج الأوزون/الأوكسجين مرة واحدة يومياً عند جرعة ١مجم/كجم)، ومجموعة معرضة لموجات صدمة جهاز تفتيت الحصوات: تلقت ٢٠٠٠ صدمة في الكلية اليمنى بمستوى طاقة ٩٠-١٠٠٪ بمعدل ٦٠ موجة صدمة في الدقيقة تحت مراقبة جهاز الاشعة. ومجموعة معرضة لموجات صدمة جهاز تفتيت الحصوات مع الاوزون الطبي: تلقت تدفق الاوزون الطبي (ما يعادل مزيج من ٩٧٪ غاز األكسجين و ٣٪ غاز الاوزون) الثابت عند ٣ لتر/ الدقيقة بتركيز أوزون قدره ٦٠ مجم/مل. و تم إعطاء مزيج الاوزون بجرعة واحدة ١ مجم/كجم/يوم عن طريق الحقن داخل الصفاق. وبعد ثلاثة أيام، تم الحصول على عينات من الدم لتقدير اليوريا والكرياتينين في مصل الدم. وقد جهزت أنسجة كلوية لقياس المالونديهايد والسوبر اوكسيد ديسميوتيزو الجلوتاثيون بيروكسيديز والفحص بالميكروسكوب الضوئي والالكتروني. وقد أُجريت تحليلات قياسية وإحصائية.

**النتائج:** كشفت مجموعة جهاز تفتيت الحصوات عن مستويات مرتفعة وملحوظه في اليوريا والكرياتينين في الدم و المالونديهايد في الانسجة. وتناقصت مستويات السوبر اوكسيد ديسميوتيزو الجلوتاثيون بيروكسيديز. وكان هناك ضمور في الكبيبات وتشوه في اقدام خلايا الرجلاء وغشاء قاعدي سميك . كما ظهرت الانابيب الكلوية مشوهة بسيتوبلازم مفرغ. وقد ارتفعت النسبة المئوية لمساحة ألياف الكولاجين و مساحة التفاعل المناعي الايجابي لاكسيد النيتريك المستحدث و بروتين الصدمة الحرارية ٧٠ ، بينما انخفض قطر الكبيبات. وتسبب الأوزون الطبي في تحسن ملحوظ من الناحيتين الهيكلية والوظيفية.

**الخلاصة:** يمكن للاوزون الطبي ان يحسن من الاصابه الحاده في الكلى بسبب التعرض لجهاز تفتيت حصوات الكلي بموجات الصدمة خارج الجسم عن طريق خواصة المضادة للاكسدة والمضادة للالتهاب.